

NASA-CR-202165

11115
11-13-78
O CIT

Final Report for NASA NCC2-5058

Single-Winged Autorotating Brake for Sensor Deployment on Mars

Principal Investigator: Ilan Kroo
NASA Ames Collaborator: Larry Lemke
Stanford Research Associate: Stephen Morris

January 1995

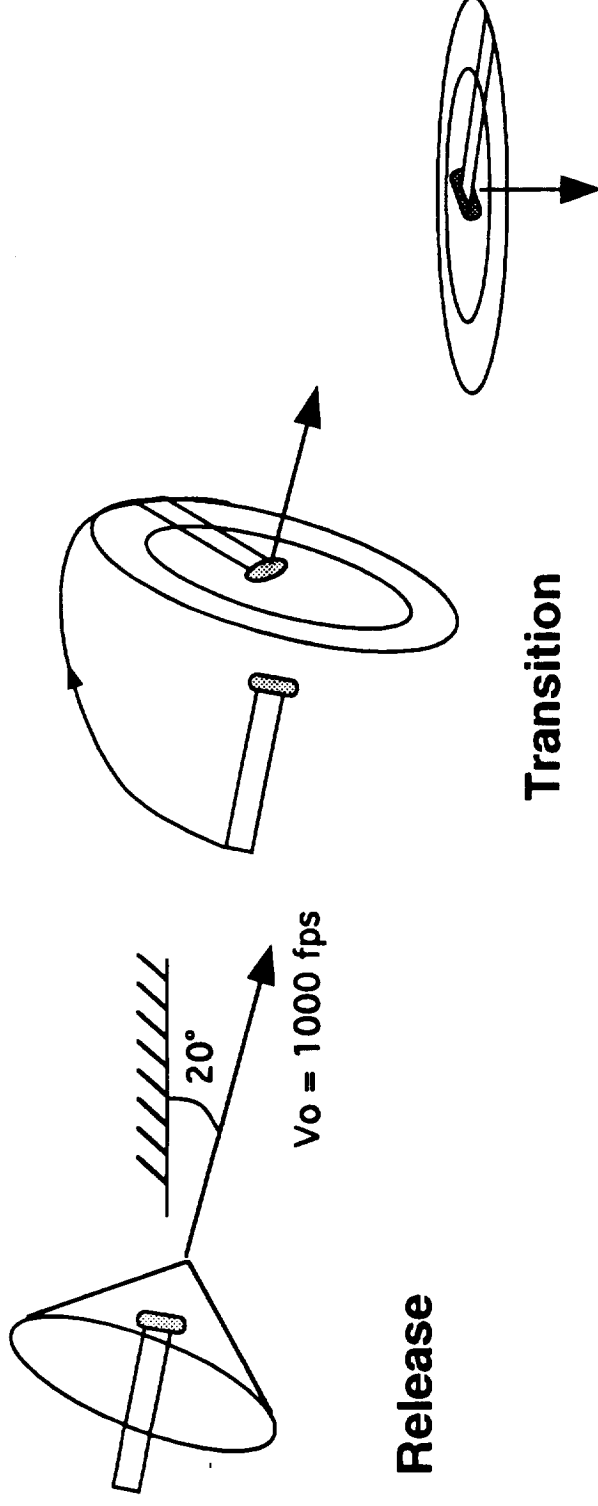
Introduction

The following pages describe the results of work performed under NASA Consortium NCC2-5058, including the development of a nonlinear simulation, results for the Martian entry problem, and a sizing study to determine whether the approach is feasible.

The nonlinear simulation is described here and results are presented for several cases using Martian and Terrestrial atmosphere models. The results show that a 2.5 kg payload could be successfully delivered to the Martian surface using this approach and the report suggests an earth-based test of the system.

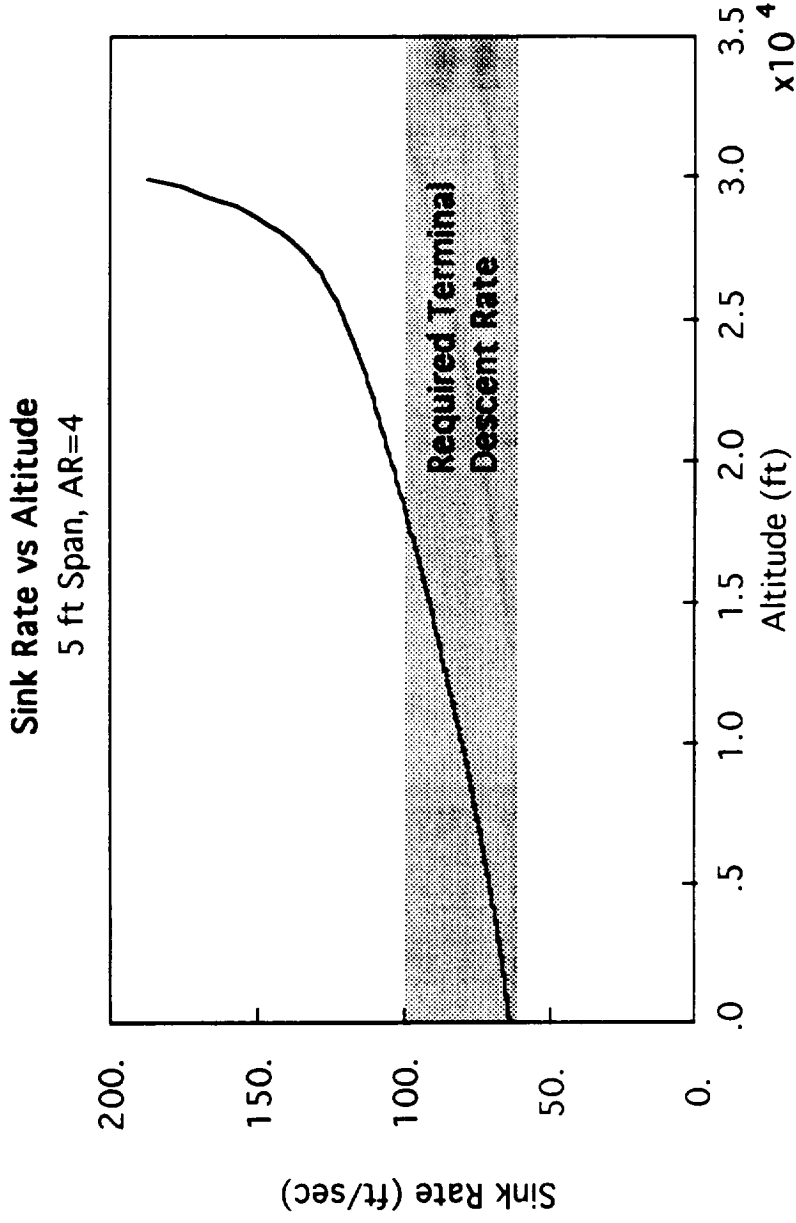
Prior to the specific analysis presented here, a theoretical study of the mechanics of autorotation was completed, and a summary of this work is also included as part of this final report.

Nonlinear Simulation



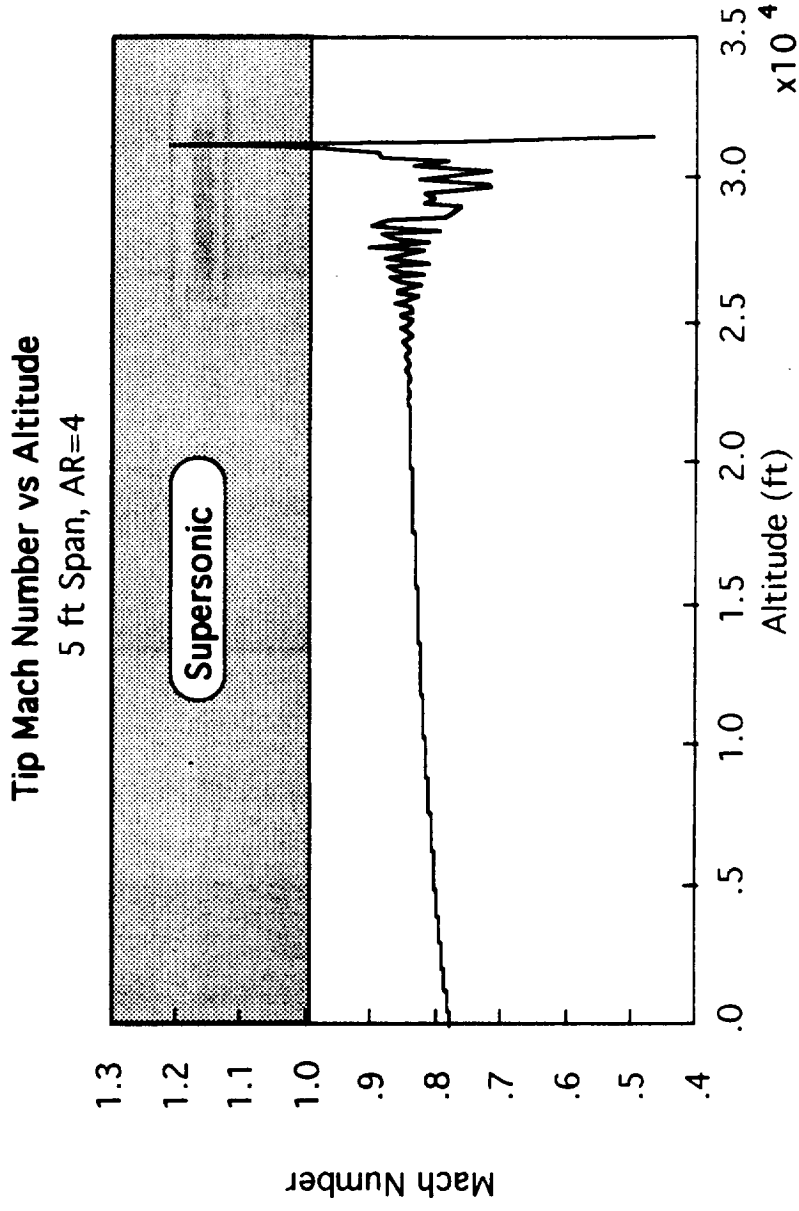
- Nonlinear 6 DOF equations of motion
- 360° angle of attack aero data (NACA 0012) w/ compressibility drag rise
- Blade-element momentum inflow model
- Mars gravity and COSPAR atmospheric model
- Simulates release, transition, and flight to touchdown

Nonlinear Simulation Results



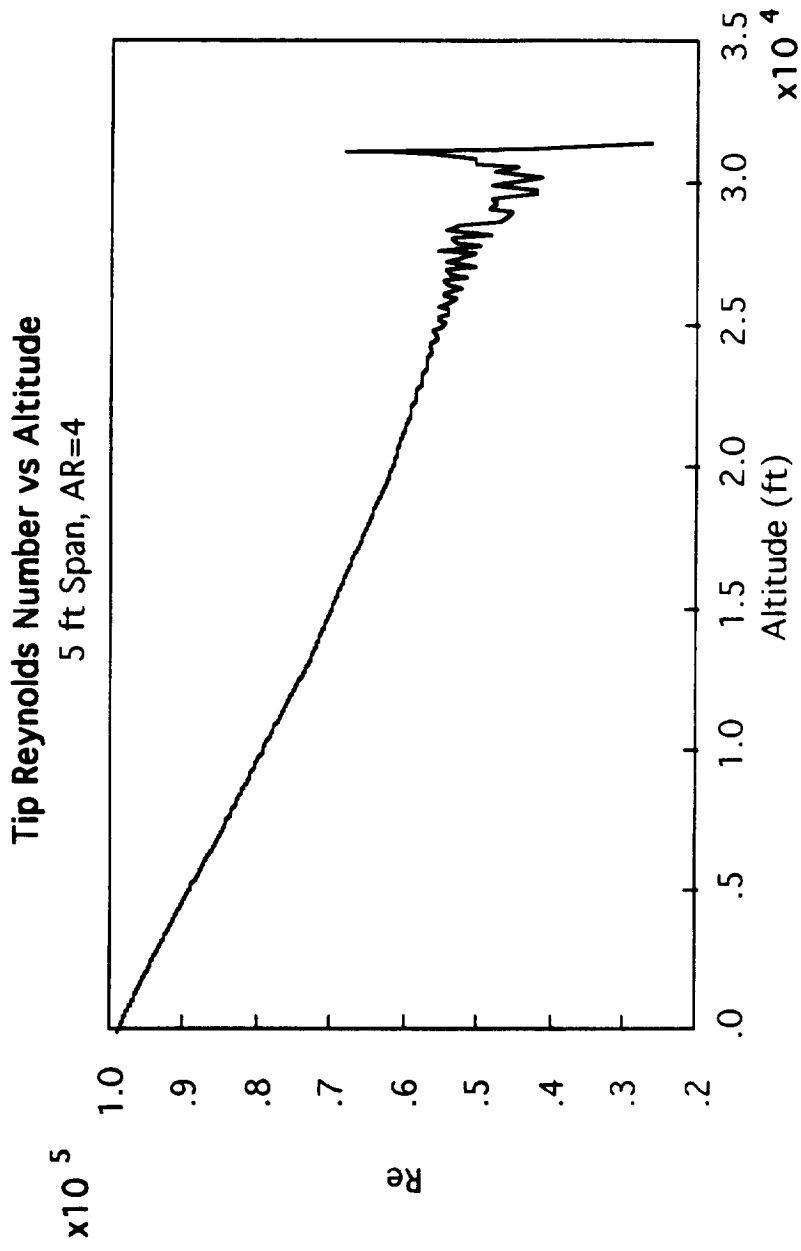
- Mass properties and CG location adjusted for stable autorotation
- Size adjusted for 65 ft/sec terminal sink rate

Nonlinear Simulation Results



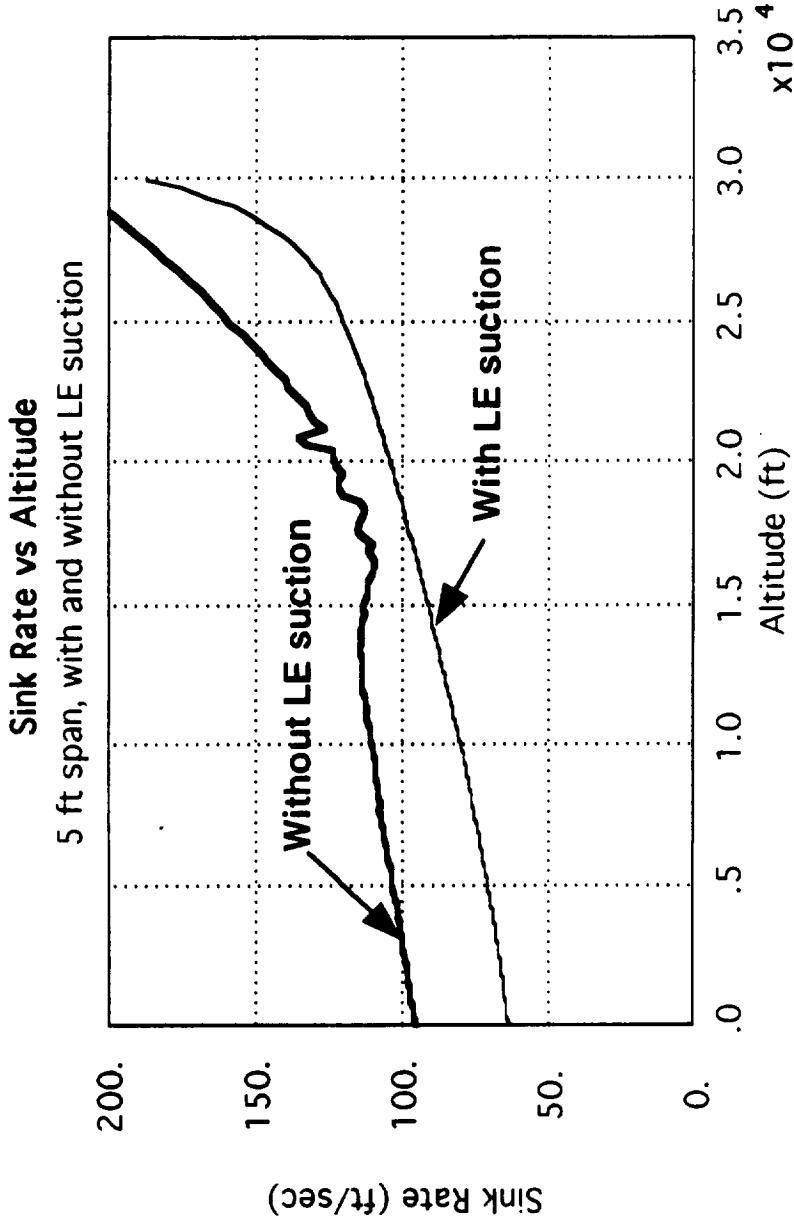
- Tip Mach Number is high subsonic in autorotation

Nonlinear Simulation Results



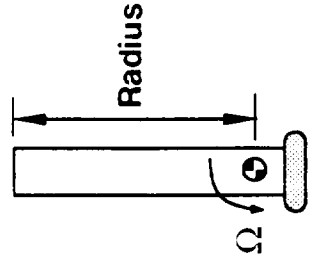
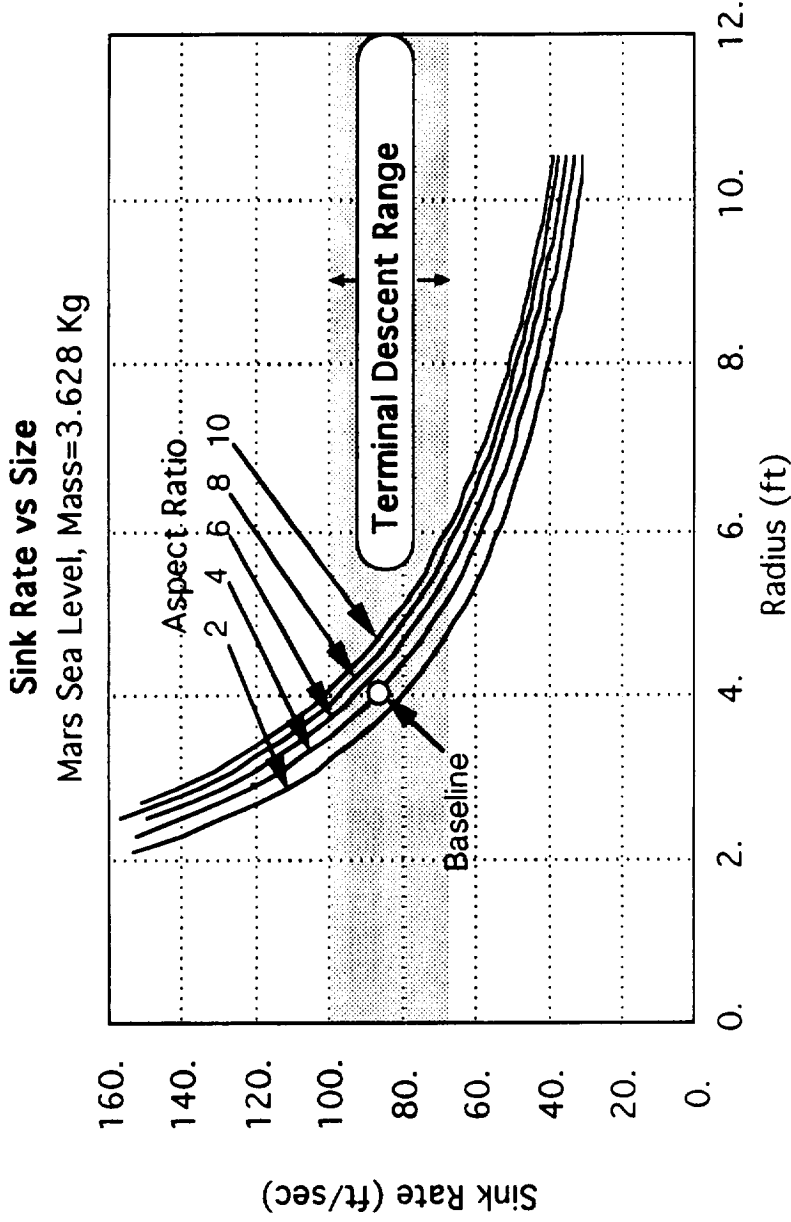
- Tip Reynolds Number is low ($< 100,000$ i.e. model airplane regime)

Nonlinear Simulation Results



- LE suction = 0 mimicks separated flow drag case (for low Re & high Mach)
- Blade trims on the edge of stall
- Terminal sink rate is 100 fps (acceptable)

Sizing Study



- Blade-element momentum model for sink rate
- Sink rate favors low blade aspect ratio, practical minimum is AR = 4
- Baseline is AR=4, radius=4 ft

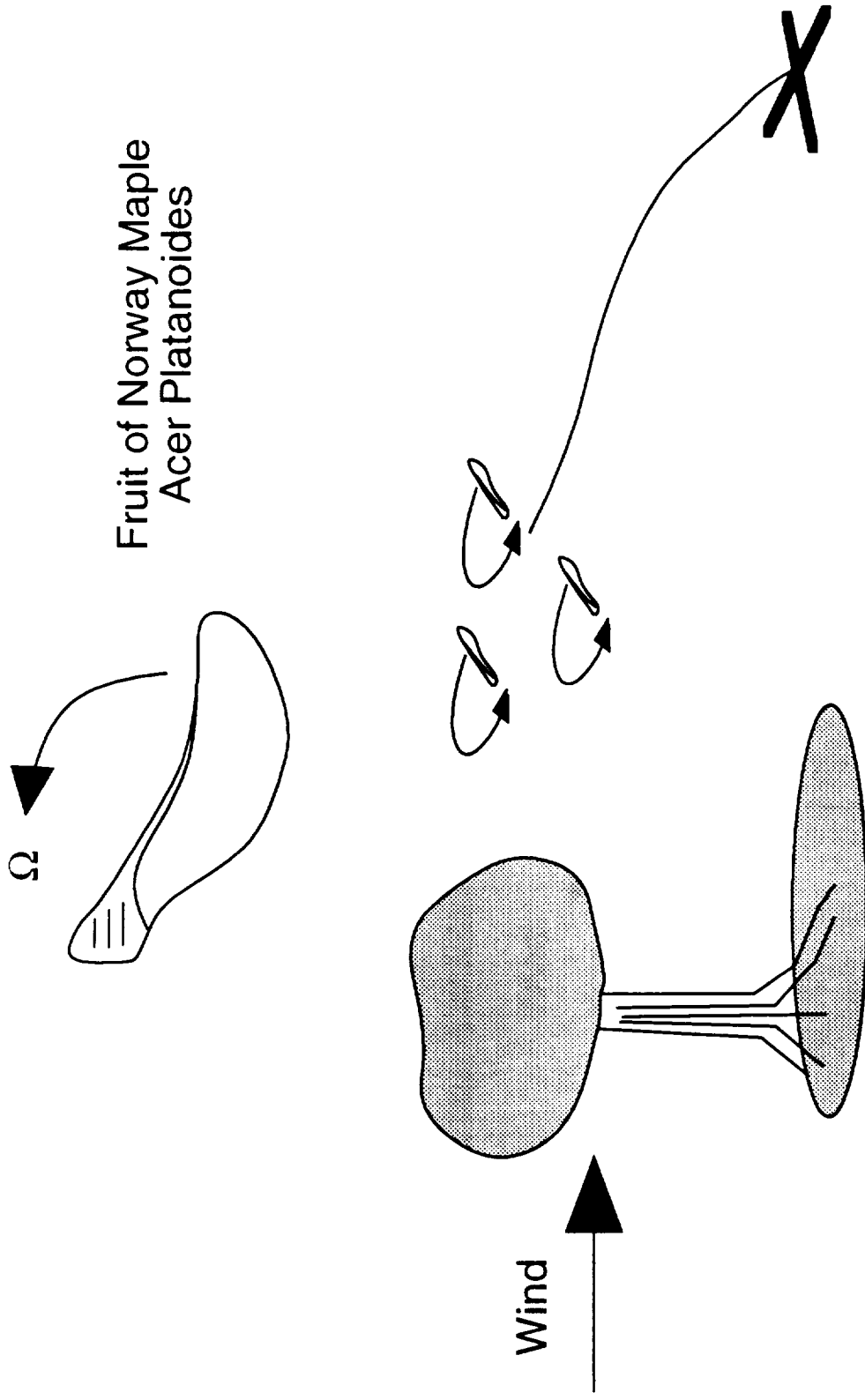
Conclusions

- **Nonlinear simulation predicts a 5 ft span and AR=4 wing delivers 2.5 kg payload successfully on Mars**
- **Primary uncertainty is low Reynolds Number / high Mach Number aerodynamics**
- **Zero leading edge suction study shows drag rise not critical for successful transition and descent**
- **Experimental tests of scaled versions in earth atmosphere necessary to demonstrate feasibility of concept**

Aerodynamics of Maple Seeds

Stephen J. Morris
Stanford University

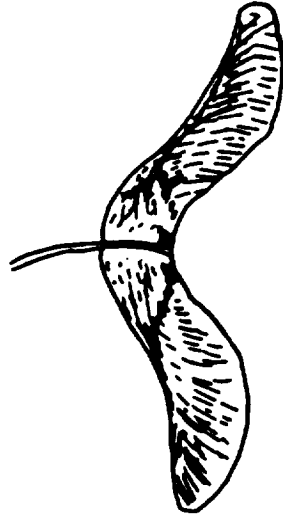
Introduction



Fruit of Norway Maple
Acer Platanoides

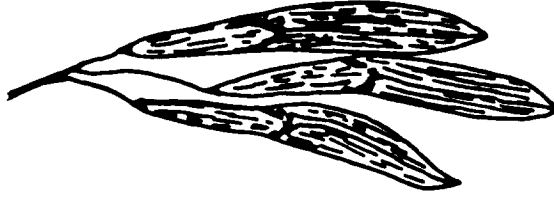
- Autorotation reduces rate of descent, seeds dispersed by wind
- Nature's 'simplest' flying machine

Seed Dispersion Using Aerodynamic Lift



(c)

Maple
(Autorotation)



(e)

Ash
(Autorotation with
long axis tumbling)



(a)

Zanonina
(Glider)

- Nature has evolved a variety of flying seeds
- Gliding is favored only when there is little surface wind

Outline

- Introduction
- Aerodynamics
 - Minimum sinking speeds
 - Blade element - momentum theory model
- Dynamics
 - Feathering axis stability
 - 6DOF simulation
 - Dynamic stability
 - Transition
- Applications
- Conclusions

Previous Work

- McCutchen, C.W.
- Norberg, R.A.
- Ward-Smith, A.J.
- Azuma, A., Yasuda, K.
- Rosen, A. , Seter, D.
- Kline, R., Koenig, W.

Minimum Sinking Speed

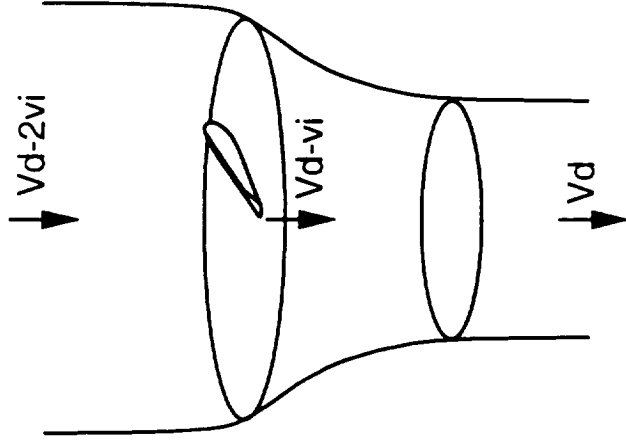
Weight = Axial Momentum Change

$$V_i = \frac{V_d}{2} - \frac{\left(V_d^2 - \frac{2W}{\rho\pi R^2}\right)^{0.5}}{2}$$

Minimum Sinking Speed

$$V_{dmin} = \sqrt{\frac{2W}{\rho\pi R^2}}$$

$$V_{i@min} = \frac{V_{dmin}}{2}$$

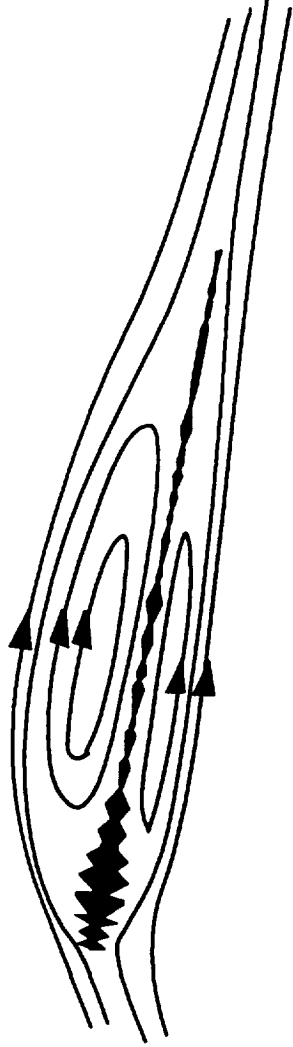


- Minimum sink rate is same as parachute with same disc loading
- Real seeds are only 10 to 35% greater than minimum

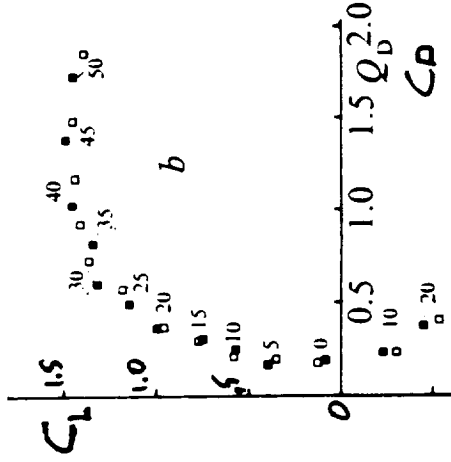
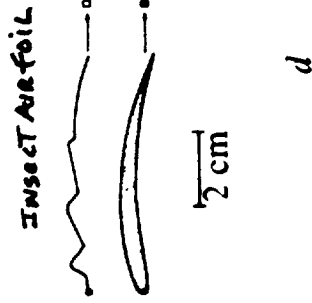
Airfoil Section Performance



Re = 1,000
(@ R=0.75)



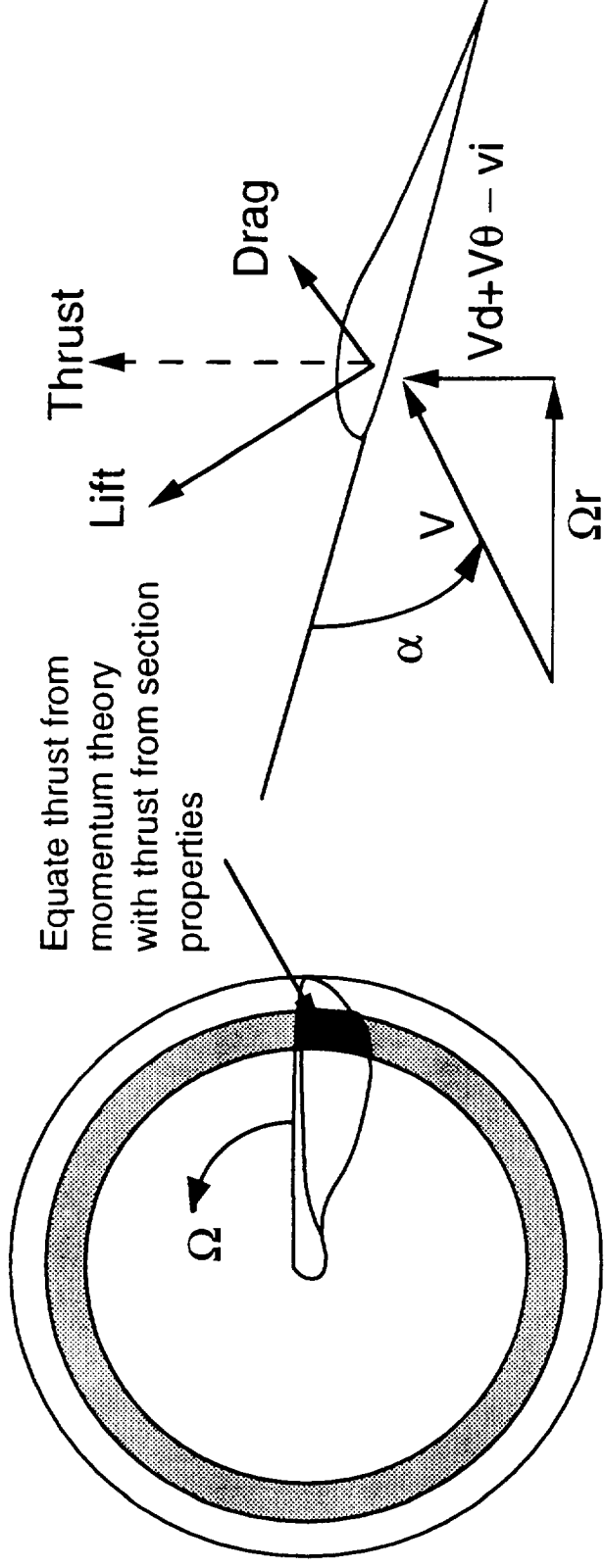
Possible Low Re Streamlines



Rees, C.
Re=450

- Airfoil is symmetric and deeply ribbed
- Jagged shape helps trip boundary layer and stabilize laminar bubble?

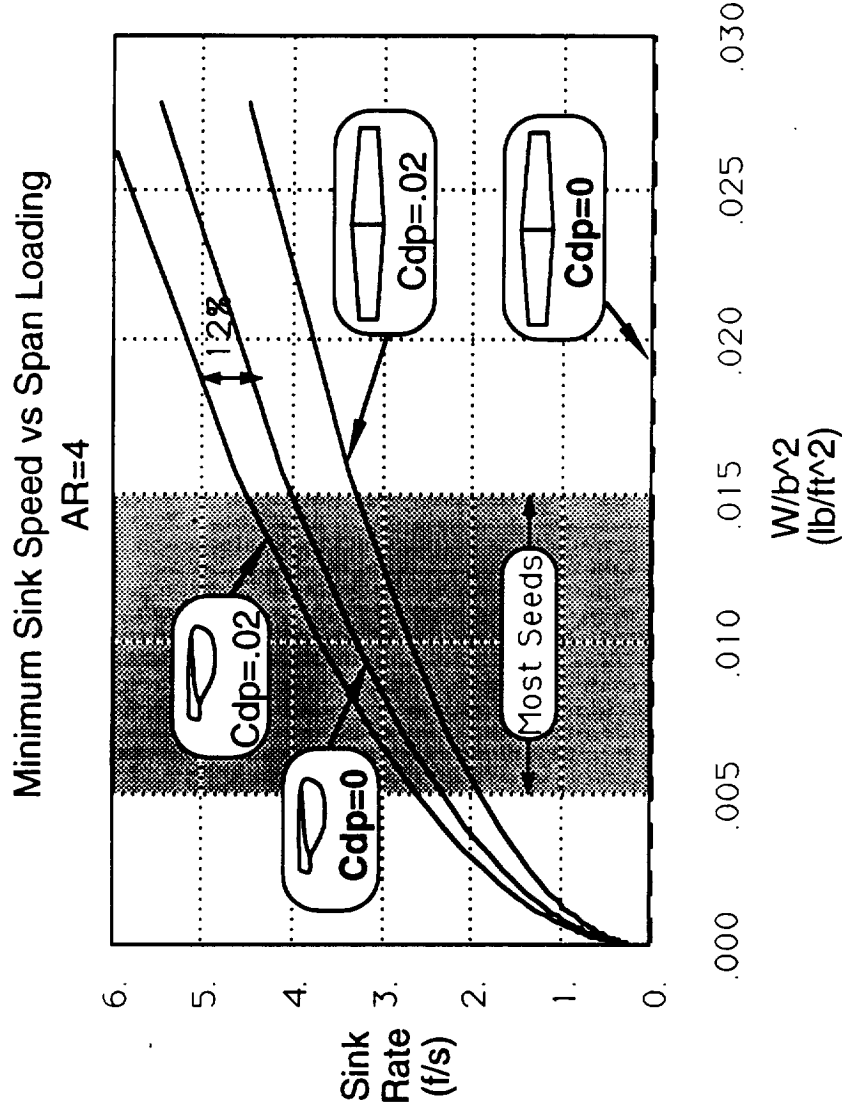
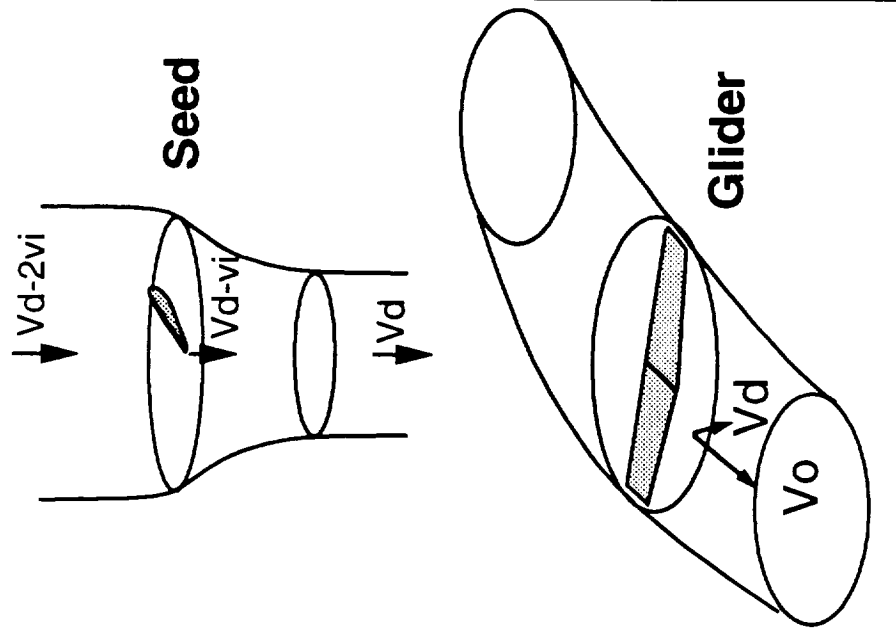
Parasite Losses - Blade Element / Momentum Theory



$$4\pi r \rho (v_i V_d - v_i^2) = q_{\text{local}} C_{L, \text{local}} \text{Chord}$$

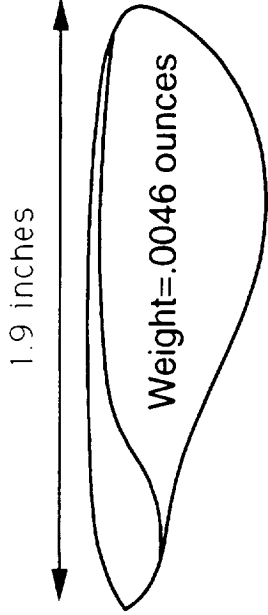
- $C_{L, \text{local}}$ is found from thrust = weight
- Solve for v_i and $C_{d, \text{local}}$

Performance with Parasite Loss

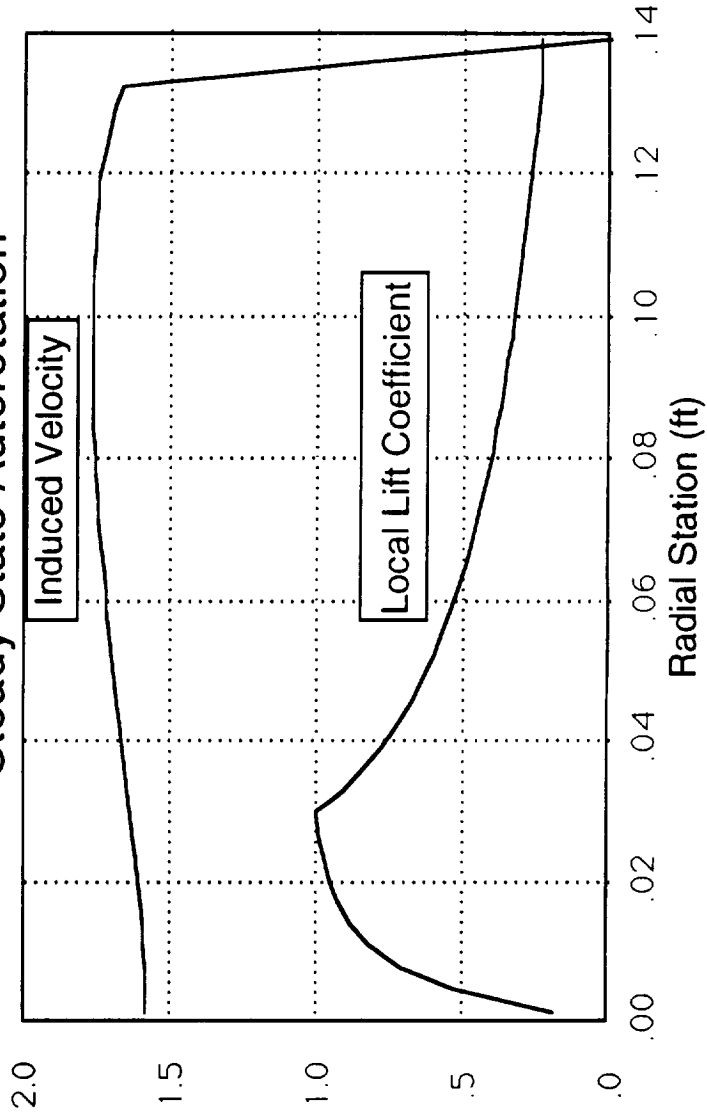


- C_{dp} not as important to seed as glider (airfoil not critical)
- Induced loss dominates because sink speed determines mass flow

Induced Losses



Steady State Autorotation



- Chord distribution produces nearly constant downwash
- Blade C_l is not large near tip

Stability



Side View

Stable Autorotation



Unstable

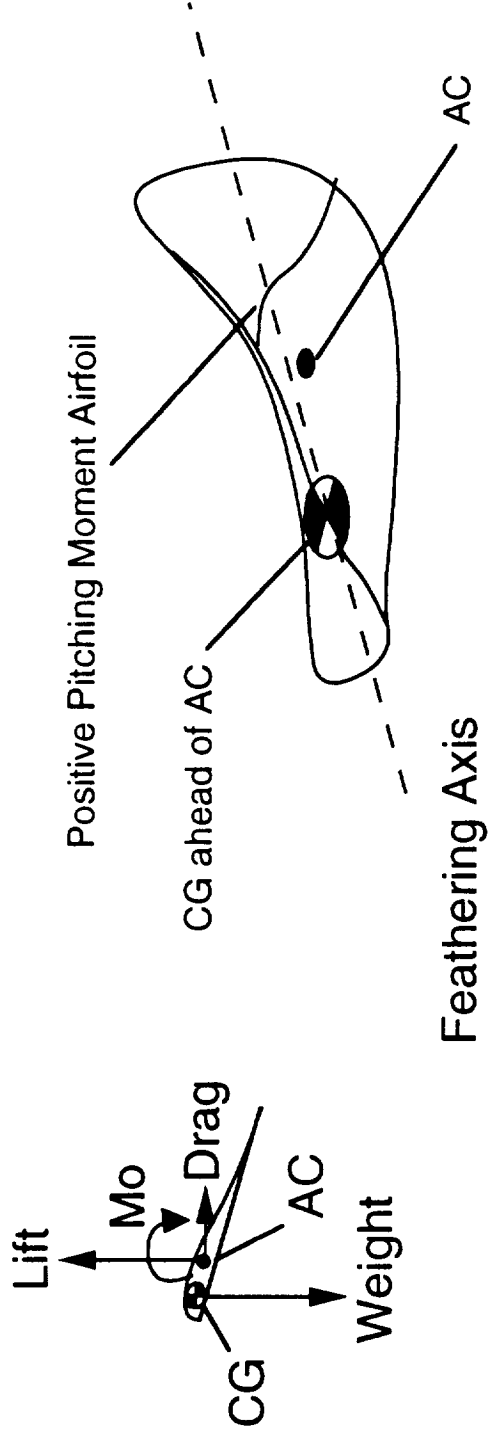
- Stability is first order important to seed dispersal, therefore evolutionary process produces robust stability

Observed Phenomenon

- Enters autorotation quickly from most initial conditions
- Autorotation not sensitive to small variations in blade camber or twist
- Autorotates with either side of blade facing up

Feathering Axis Stability Previous Theory for Maple Seed

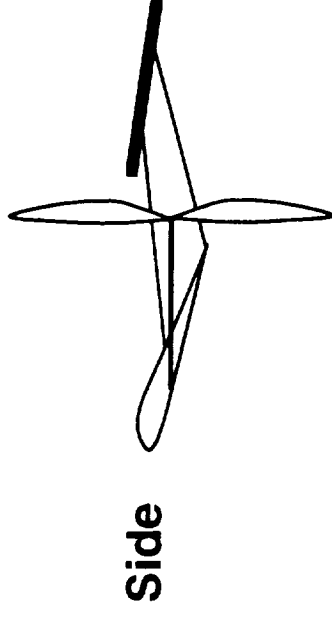
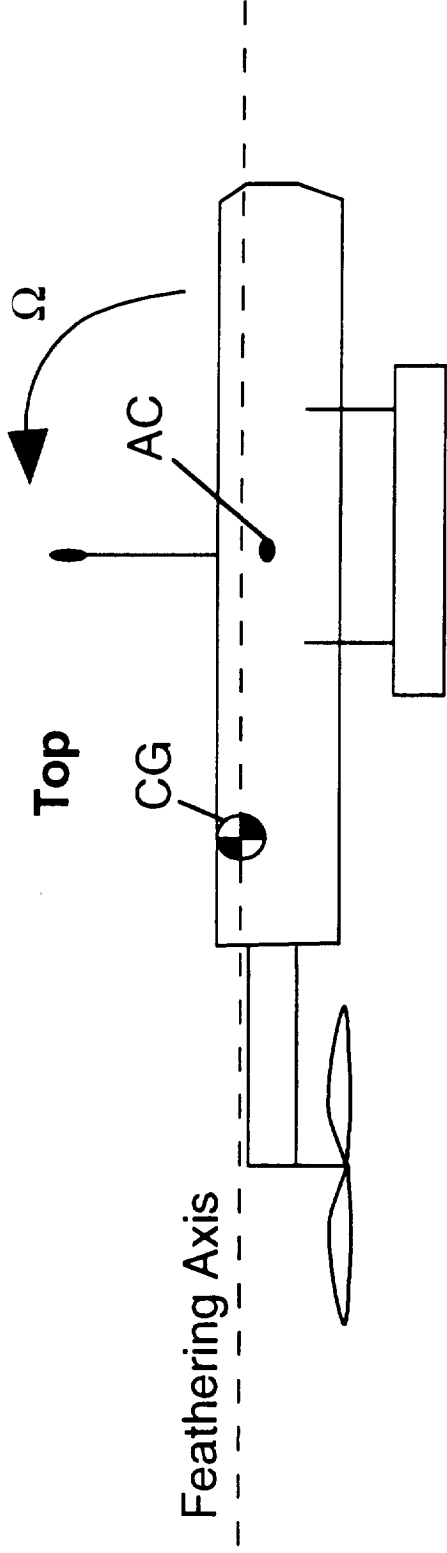
(McCutchen, C. 1954, Norberg, R.A. 1973)



- Seed has static aerodynamic pitch stability about feathering axis due to CG location and airfoil reflex
- Governing pitch equation of motion is: $\ddot{q} = \frac{M_{cg}}{I_{yy}}$
- Seed is like flying wing airplane in a tight circling flight path

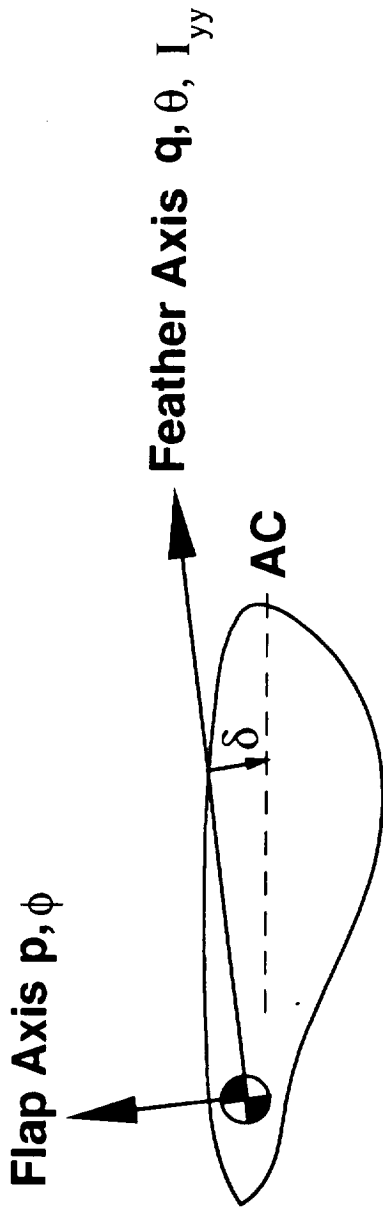
Example of an Aerodynamically Stabilized 'Seed'

C. W. McCutchen Wing



- Static aerodynamic pitch stability
- Trims at a fixed angle of attack (power or glide)
- Will only fly with proper side upward

Feathering Axis EOM



Trim

$$\int_{\text{root}}^{\text{Tip}} C_{q_{\text{local}}} [-\delta C_{L_{\text{local}}} + (C_{m_0} + C_{mq}(q - \Omega\phi))] C] ds = I_{yy} (\Omega p + \Omega^2 \theta)$$

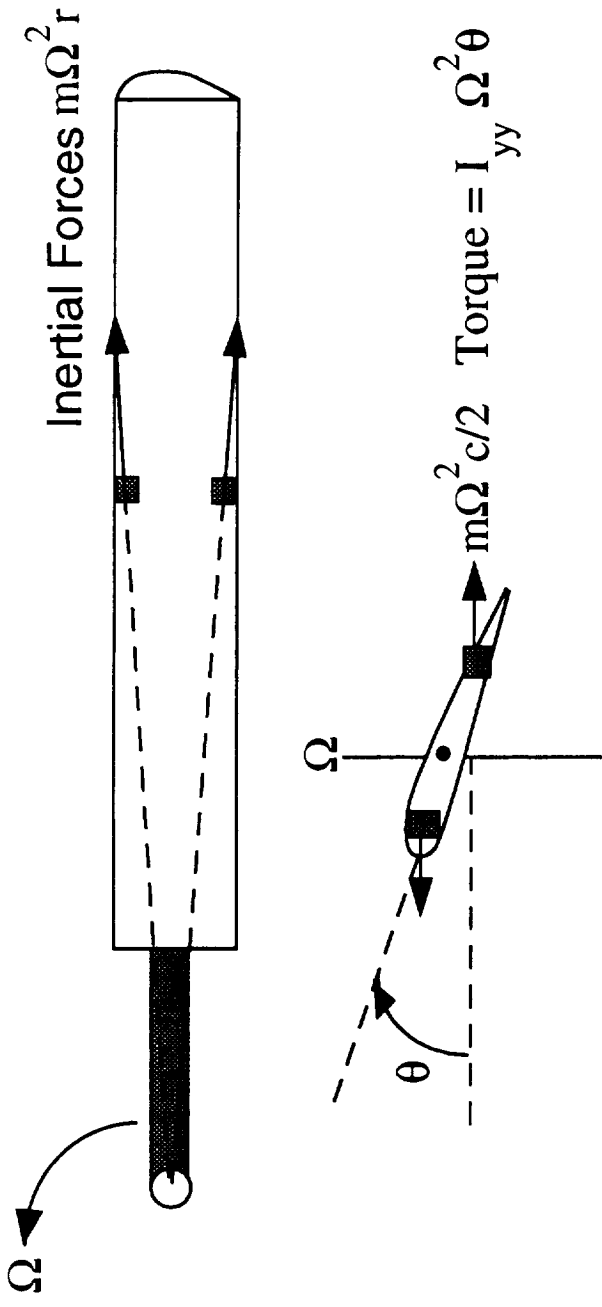
Lift	Airfoil	Pitch Rate	= Gyro Pitch
@ AC	Cmo	Damping	Coupling Inertia
(±)	(0)	(-)	(small) (-)

Static Stability

$$\frac{\partial \dot{q}}{\partial \theta} = \frac{1}{I_{yy}} \int_{\text{hub}}^{\text{tip}} C_{q_{\text{local}}} [-\delta C_{l\alpha}] ds - \Omega^2$$

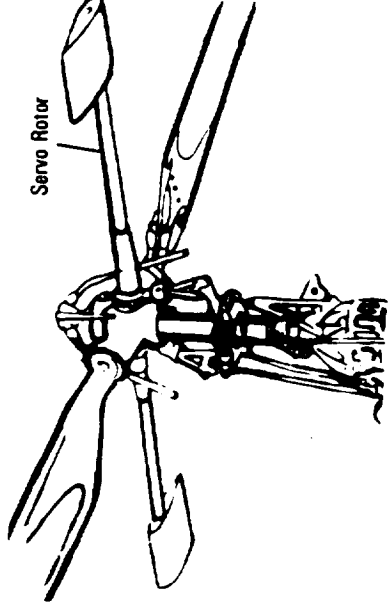
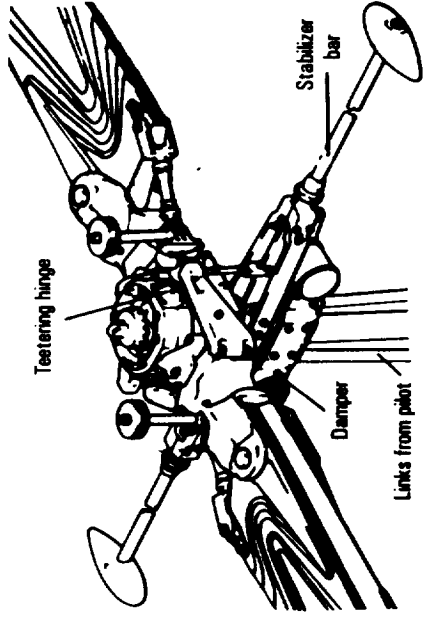
Lift	Pitch
@ AC	Inertia
(±)	(-)

Feathering Axis EOM (cont)



- When Ω is large pitch inertia term $I_{yy} \Omega^2$ dominates aerodynamic terms
- C_{mo} not required to trim
- Feather axis ahead of AC not required for stability
- Motorized seed will not climb

Comparison with Helicopter Rotor

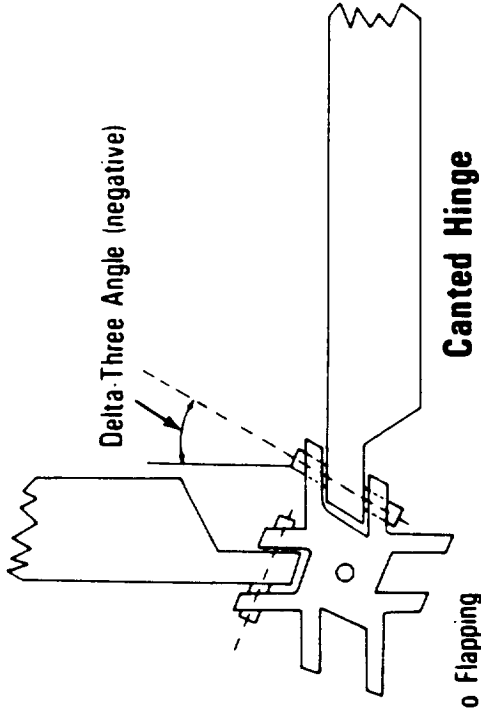
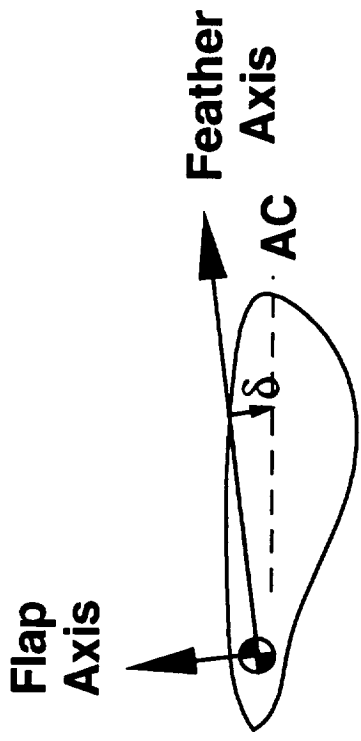


Bell Stabilizer Bar Stabilizer Bar with Hiller Paddles

- Blades are mechanically stabilized about feathering axis
- Bell Stabilizer bar provides attitude feedback for hover stability
- Hiller paddles allow stabilizer bar to be tilted for control

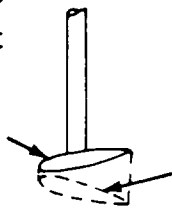


Comparison with Helicopter Rotor (cont)



Rotation of Principle Axes

Pitch with No Flapping



Pitch with Flapping

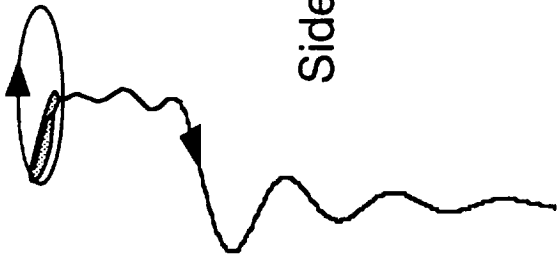
"Delta 3" Hinge
Pitch/Flap Coupling

- Rotation of principle axes from AC couples flapping motion with angle of attack change (feathering)

Numerical Simulation of Autorotating Seeds

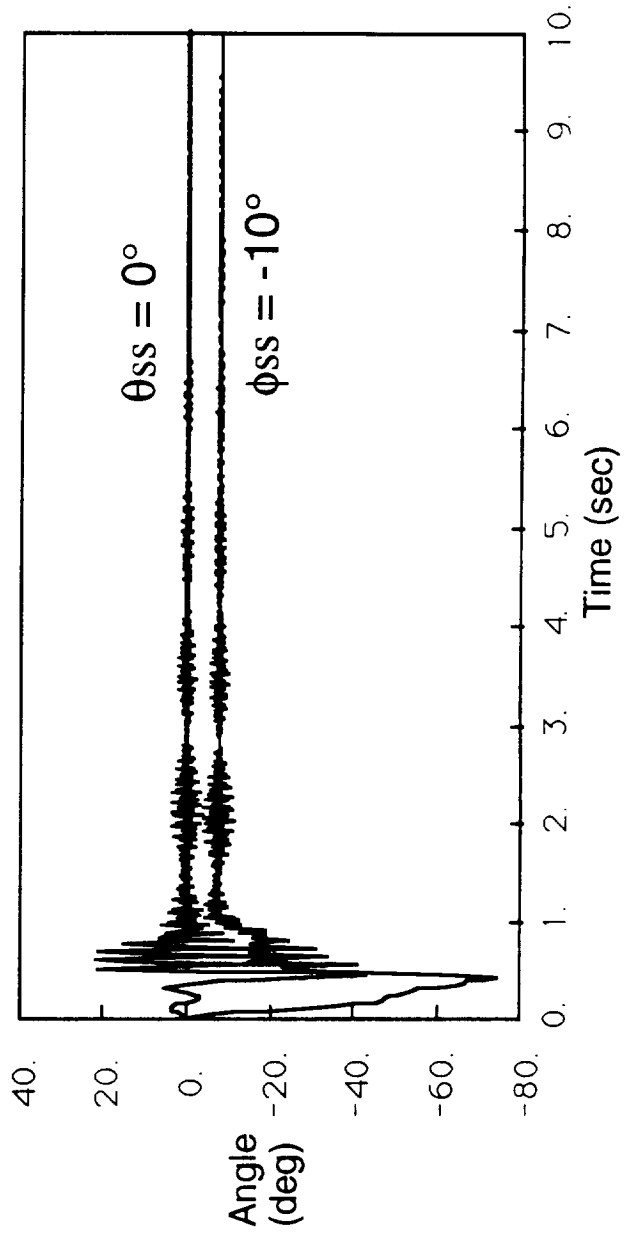
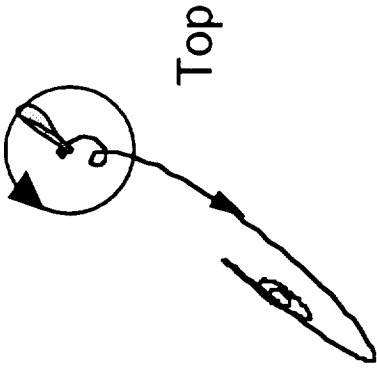
- All kinematics are six DOF and nonlinear
- Full inertia tensor is retained
- Aerodynamic model is quasi-steady strip theory with blade element - momentum theory used for calculating axial induced velocities
- All velocities due to rotary motions about any axis are considered
- 2-D airfoil section data used for C_l & C_d at each blade station (for 360° alpha range)
- 4th order Runge-Kutta integration

Simulation Results



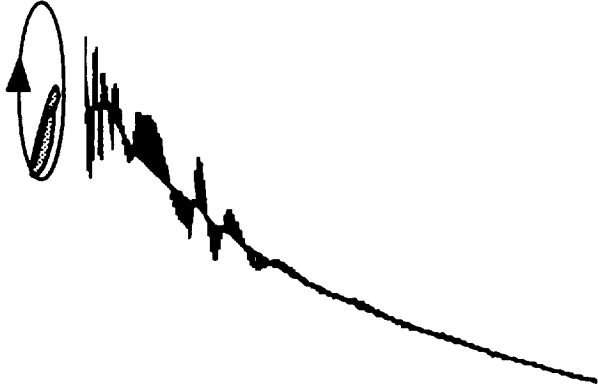
Fruit of Norway

Mass Center Motion



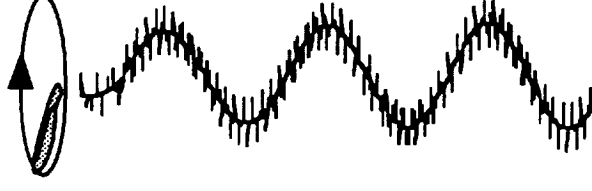
Dynamic Stability - Effect of Pitch Inertia

Side View



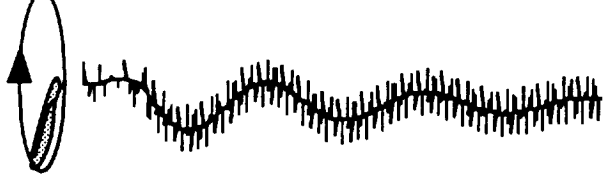
$$I_{yy} = 1 \times 10^{-10}$$

$$Vd = 50 \text{ f/s}$$



$$I_{yy} = 3 \times 10^{-9}$$

$$Vd = 2.5 \text{ f/s}$$



$$I_{yy} = 5 \times 10^{-9}$$

$$Vd = 2.5 \text{ f/s}$$

- Increased pitch inertia dynamically stabilizes autorotation descent

Dynamic Stability - Effect of CG location

Side View



$$X_{CG} = -.015 \text{ ft}$$



$$X_{CG} = -.020 \text{ ft}$$

- Slightly aft CG increases dynamic stability

Advancing Blade "Flap Back"

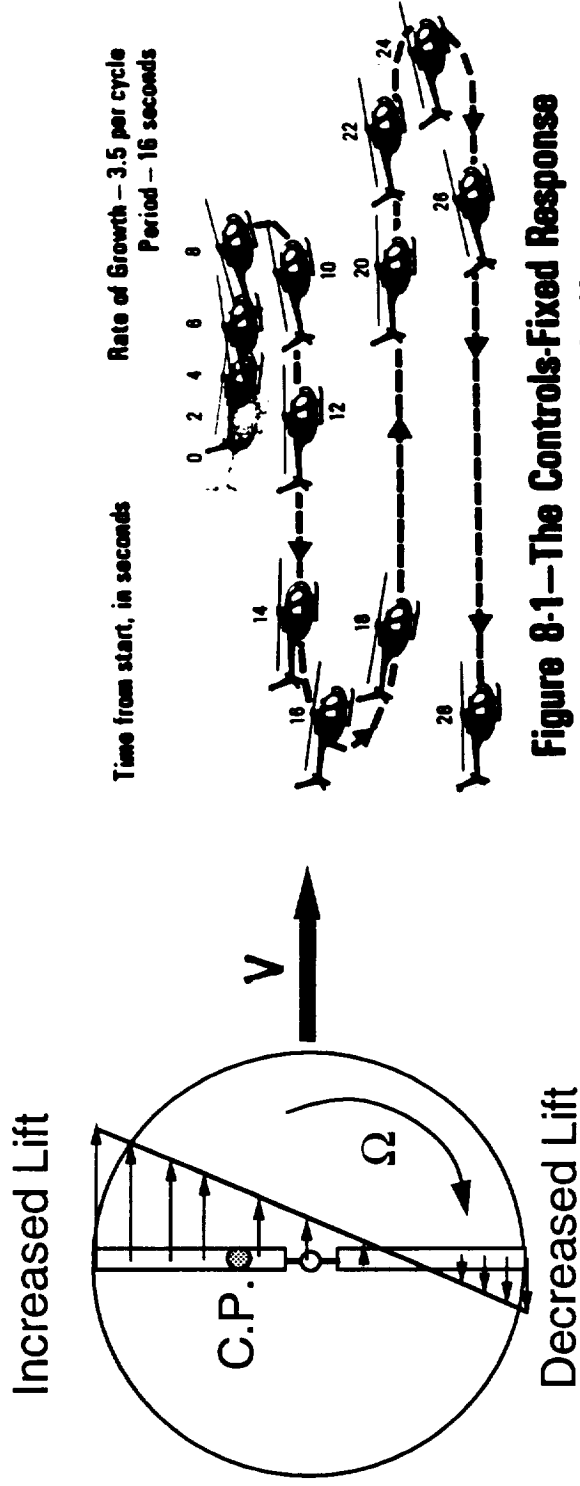
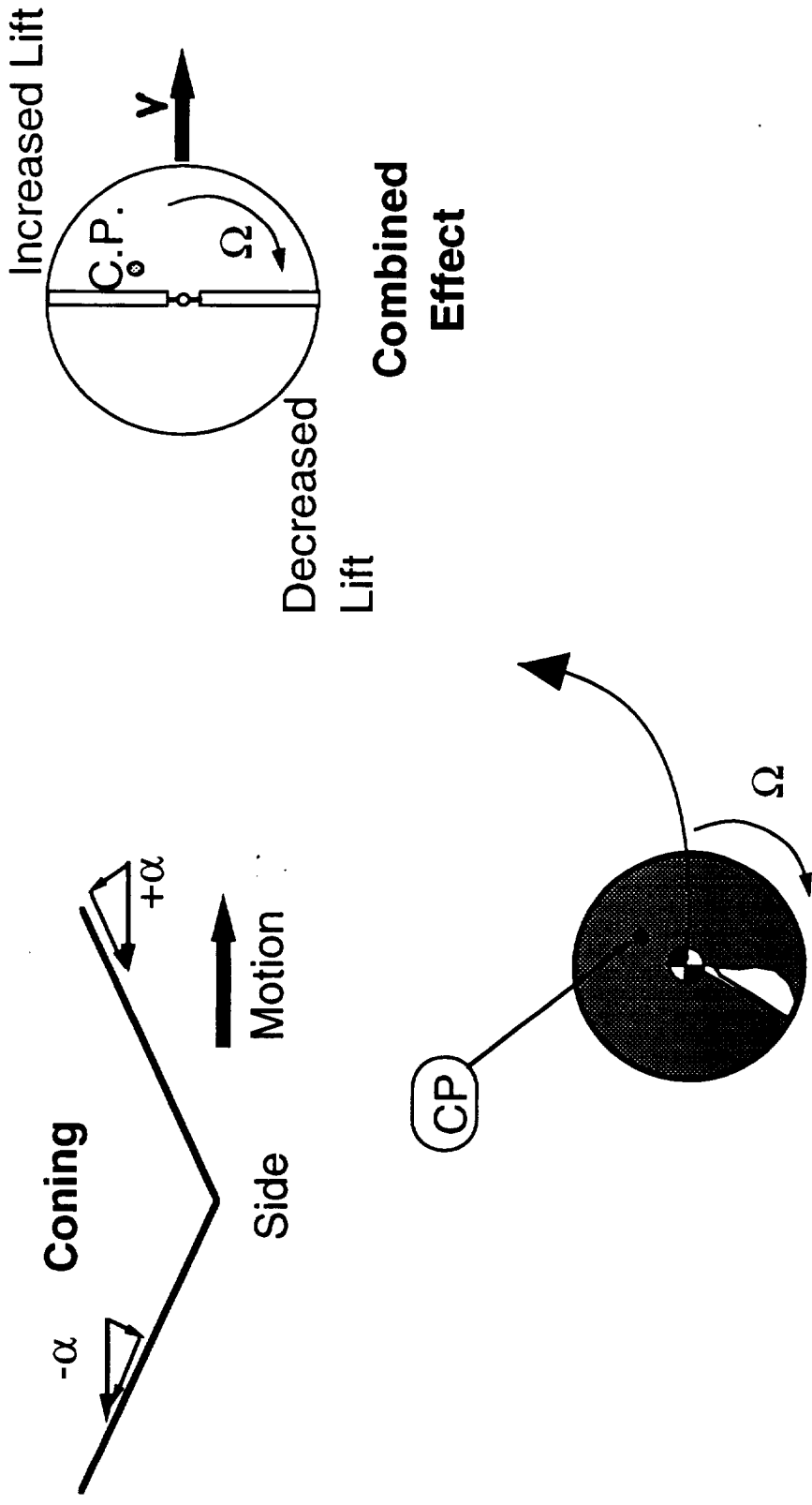


Figure 8-1—The Controls-Fixed Response To a Disturbance in Hover

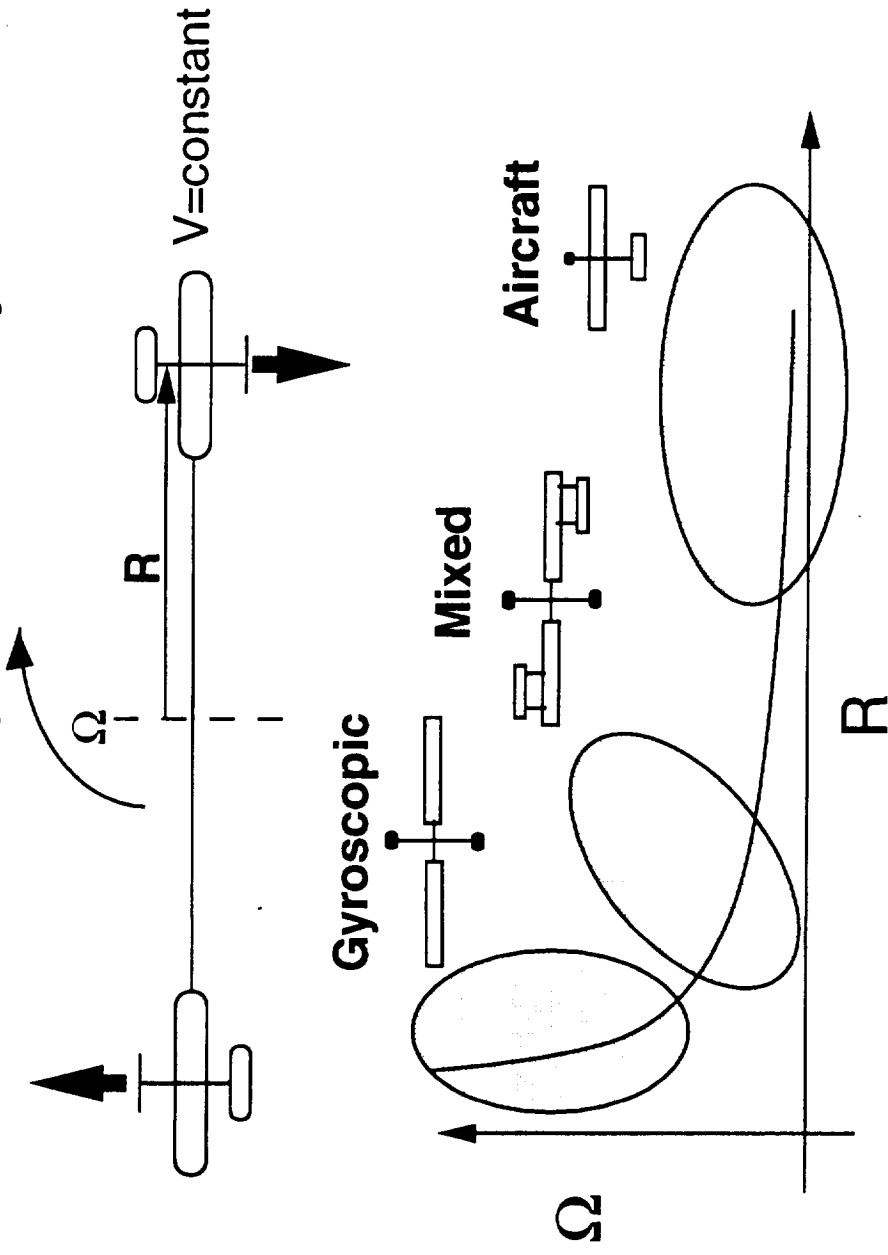
- Motion is driven by rotor "flap-back" when helicopter moves forward
- Stabilizer bar can reduce hover dynamic instability

Coning Induced Lift Change



- Motion is a left circle due to advancing blade and coning effects
- Dynamic stability determines whether motion damps out

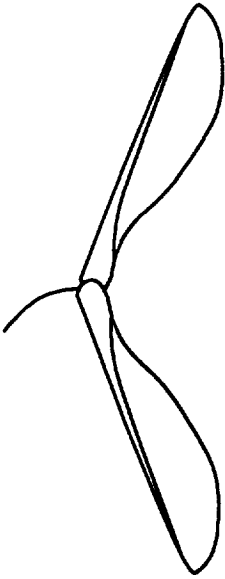
Types of Dynamic Stability



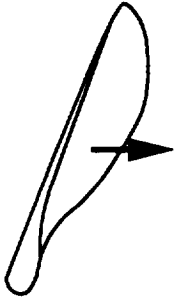
- Gyroscopic stability dominates at small R and large Ω for fixed disc loading

Transition: Falling to Autorotation

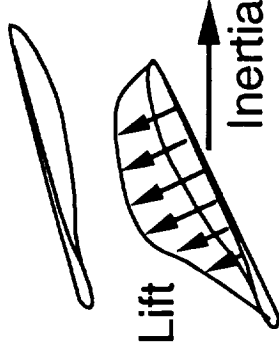
Seed on Tree



Falling T.E. First
Begin to pitch and yaw



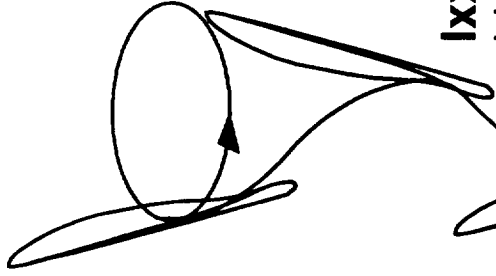
Rotates Through Unstalled α
Gyroscopic forces flatten seed
motion



Autorotation Begins
Rotation speed increases
Blade pitch flattens
Dynamic stability damps transients

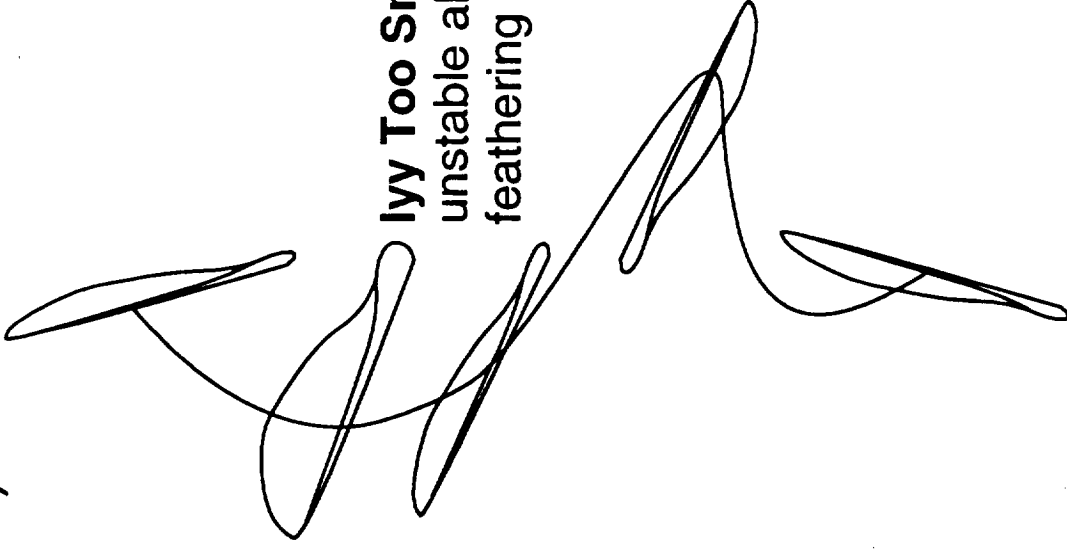


Transition (cont)

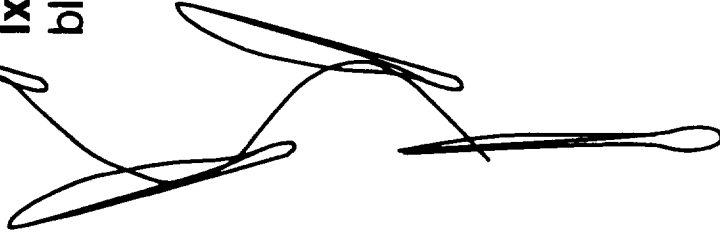


Ixx Too Small
blade coning too high

Iyy Too Small
unstable about feathering axis

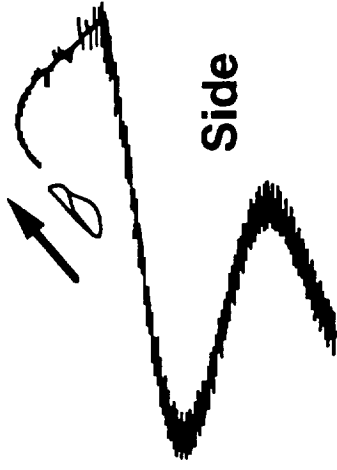


Ratio of Ixx to Iyy is Critical

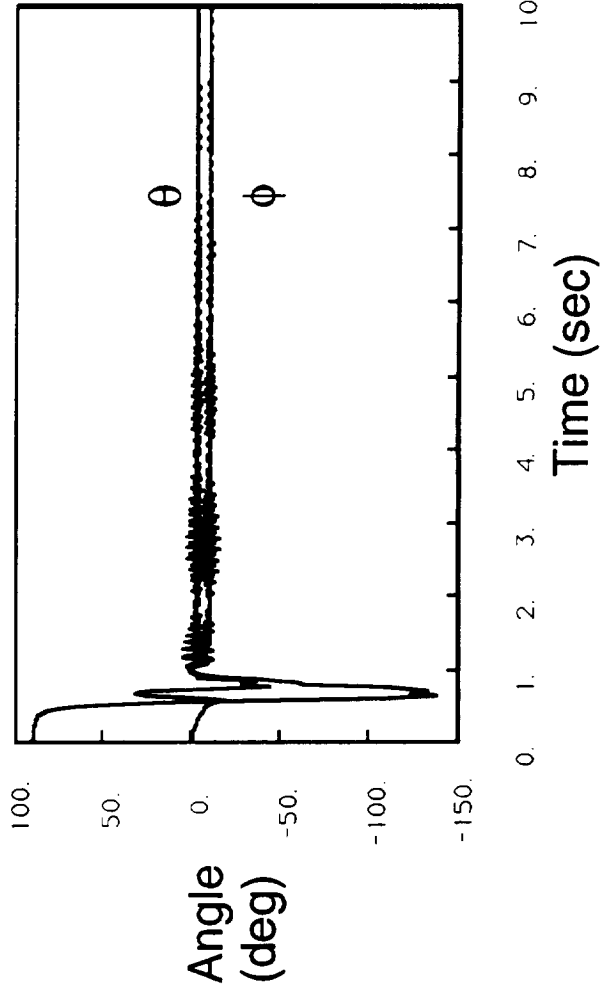


Transition - Simulation Results

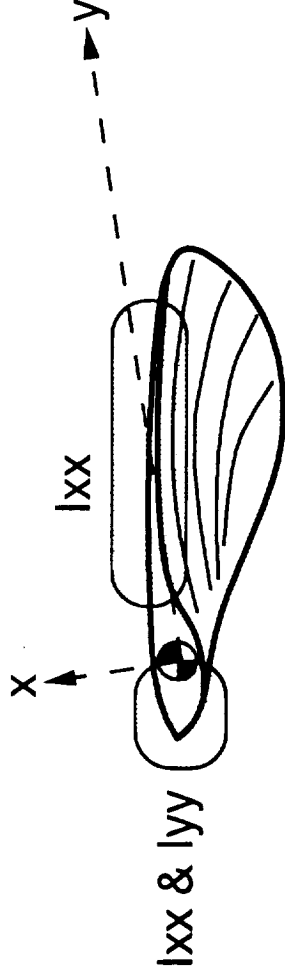
Seed Thrown Upward into Air



Angle vs Time



Transition - Notes from Simulation Work



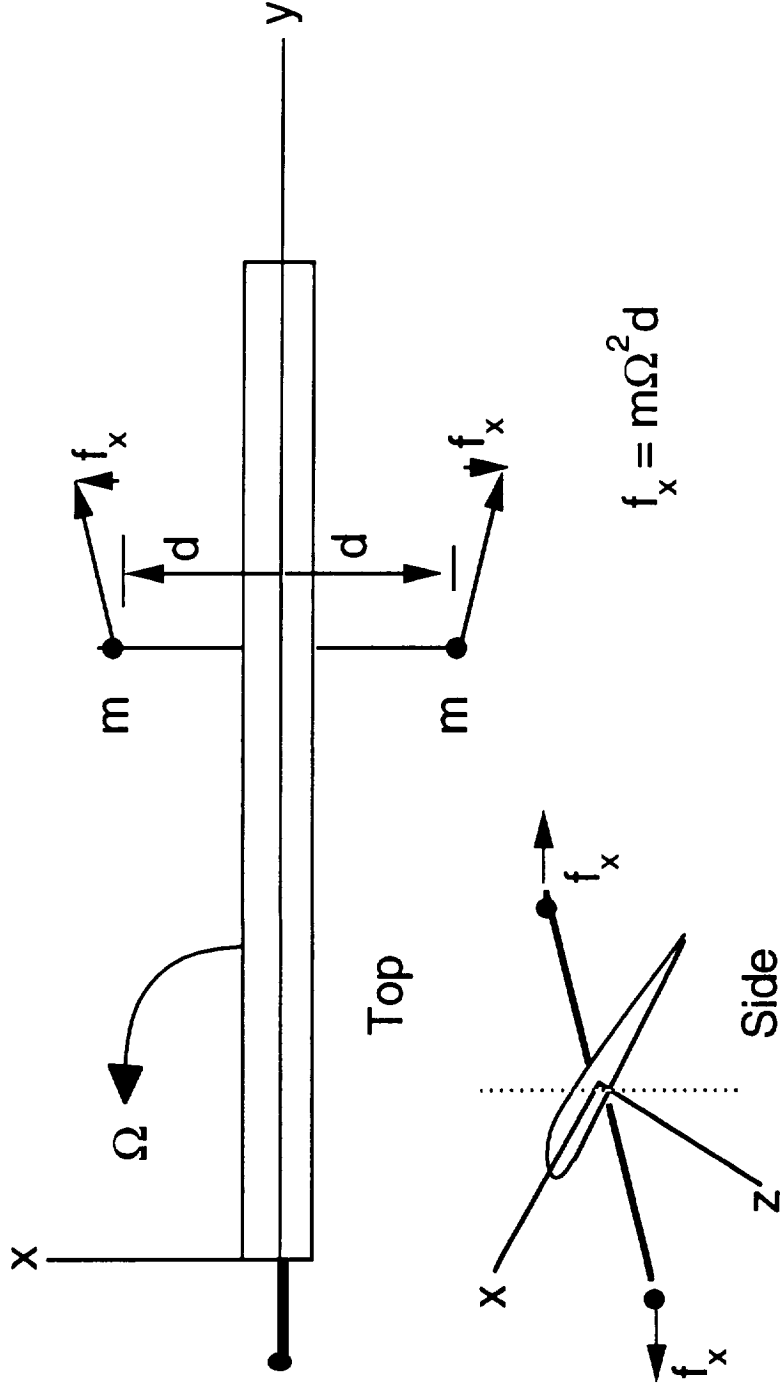
- Vacuum trajectory is unstable for disturbances about intermediate axis of inertia
- Small variations in camber and twist help excite rotary motion
- Ratio of I_{xx} to I_{yy} is critical for autorotation to develop
- Some initial conditions result in difficult transition

Application of Gyroscopic Feathering Axis Stability for Advanced Rotor Design

Areas where gyroscopic effects may be helpful

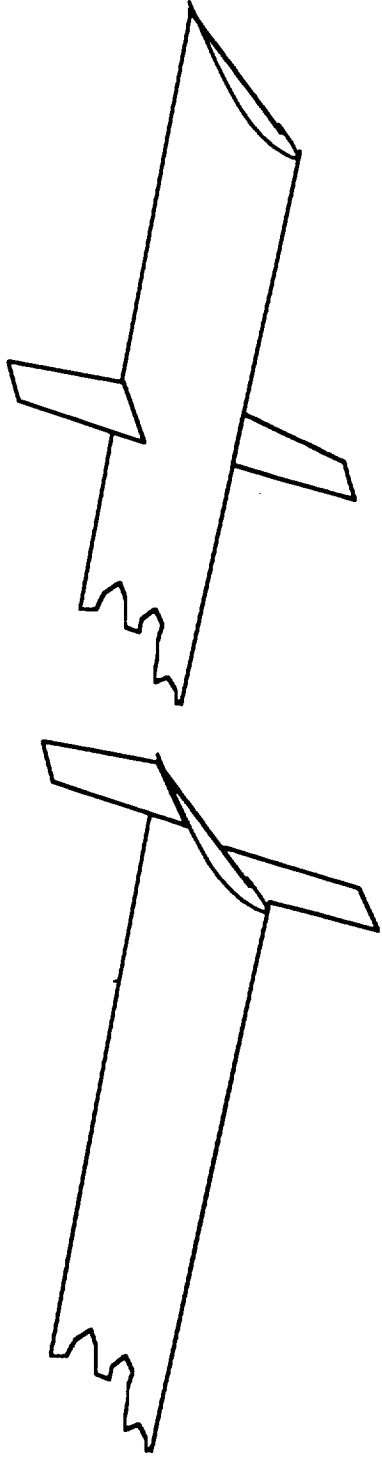
- Permit use of efficient airfoil sections at rotor tip by gyroscopically relieving torsional moments
- Improve aeroelastic stability of bearingless rotor designs which use trailing edge flaps for blade pitch control

Airfoil Pitching Moment Reduction Using Centrifugal Force



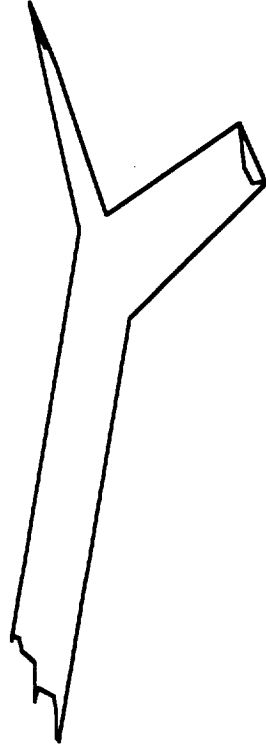
- Ixz term produces a nose up moment that can counter airfoil camber effects
- Allows transonic airfoils with large negative pitching moments at rotor tip
- Reduces torsional aeroelastic problems

Possible Rotor Designs for Tailored Ixz



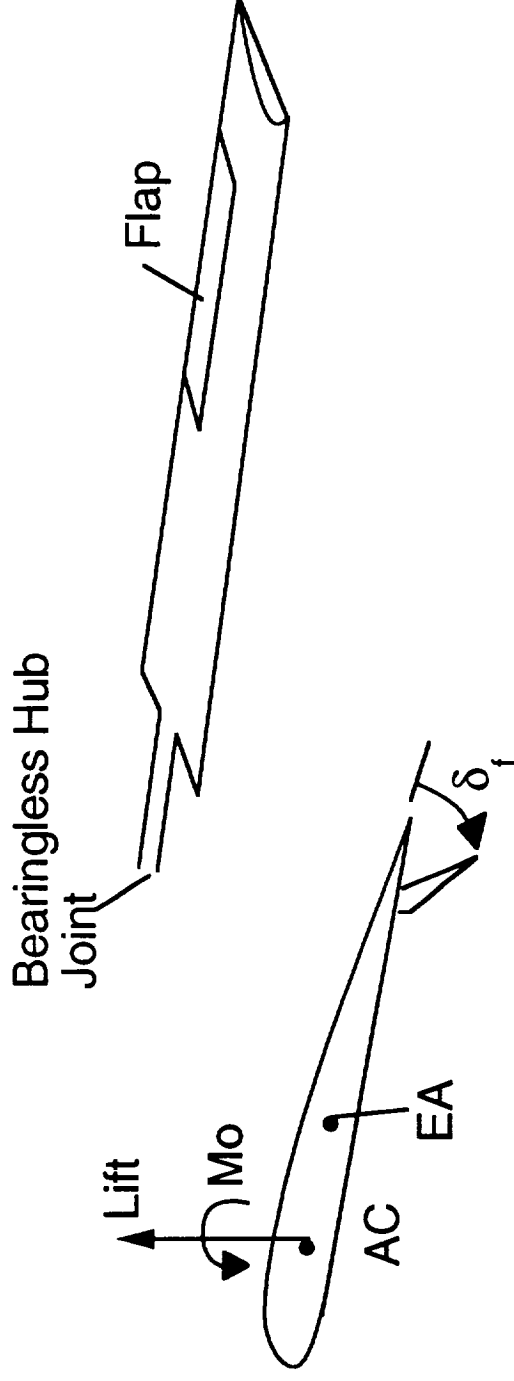
Winglet Tip

Inboard Winglet Tip



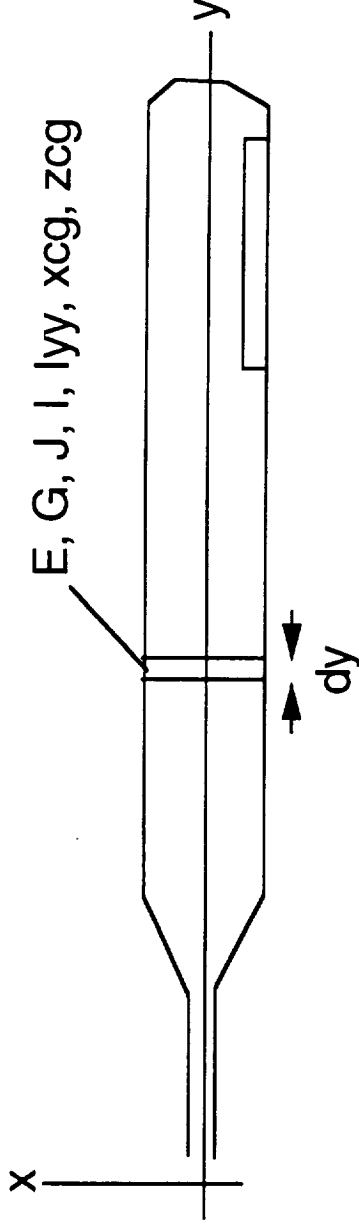
Split Tip

Gyroscopic Stability for Feathering Axis of a Bearingless Rotor Design



- Moment trim with efficient flap deflection implies EA behind AC
- Aeroelastic stability is low
- Gyroscopic stiffening can significantly improve aeroelastic stability

Integrated Design of Advanced Bearingless Rotor



- Simultaneously solve for mass and stiffness distribution that yields a stable, controllable rotor with the minimum weight or power required
- Include mass and stiffness parameters in the nonlinear optimization that minimizes:

$$J = \int_0^{\infty} (\dot{x}^T Q x + u^T R u) dt + K(\text{weight}) + F(\text{Power})$$

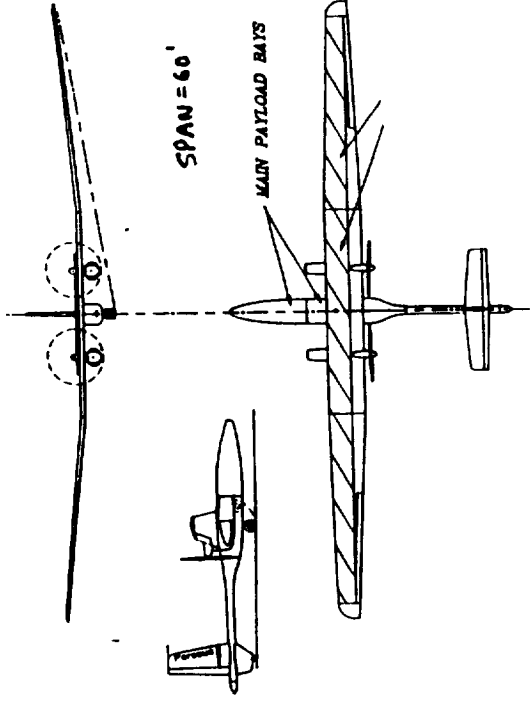
J = total cost function

x = rotor dynamic state vector

u = rotor control vector

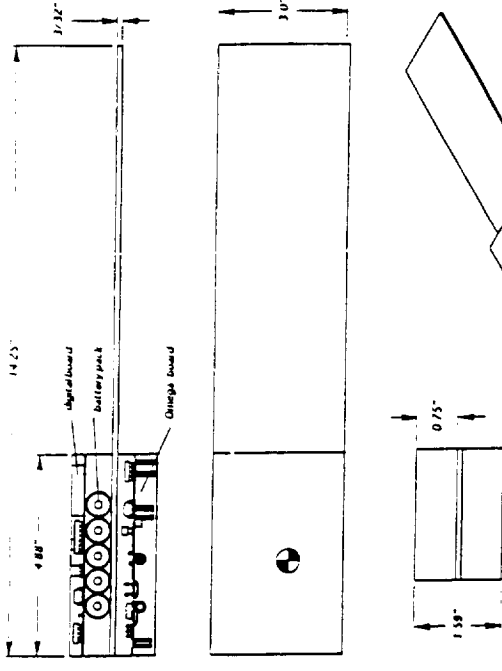
Applications of Single-Winged Autorotating Devices

Gyrosonde



Perseus

High Altitude Research Aircraft



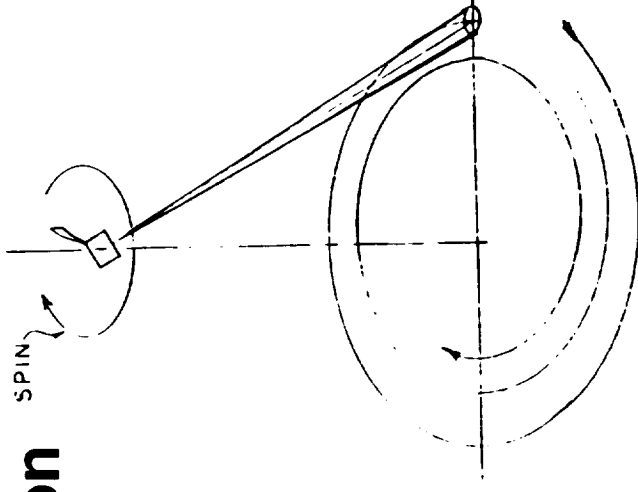
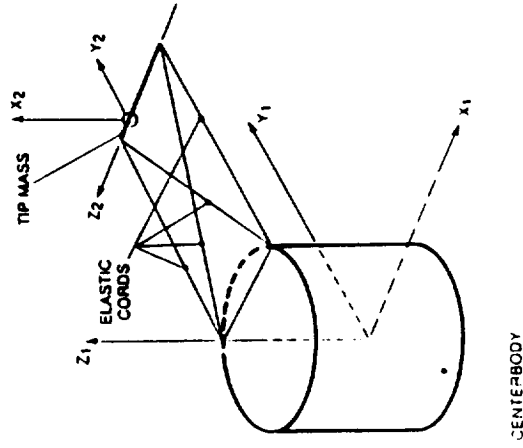
Gyrosonde

- Atmospheric sensing device relays position, pressure, temperature, and humidity information
- Replaces parachute dropwindsonde
- Packing efficiency, robust deployment, cheaper to manufacture

Applications (cont)

Samara-Winged Decelerator

Submunition



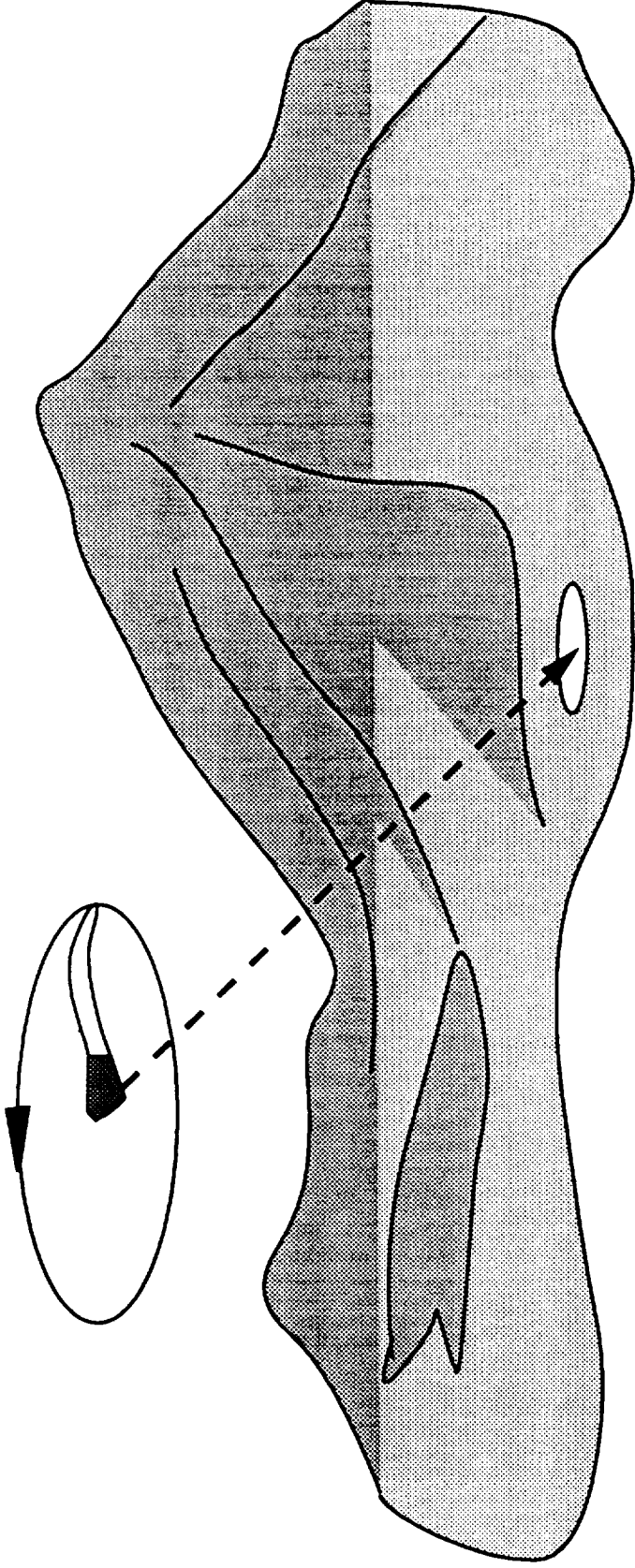
Submunition

Operation

- Foldable, gyroscopically stiffened wing
- Rotary motion used to scan battlefield with a sensor

Applications (cont)

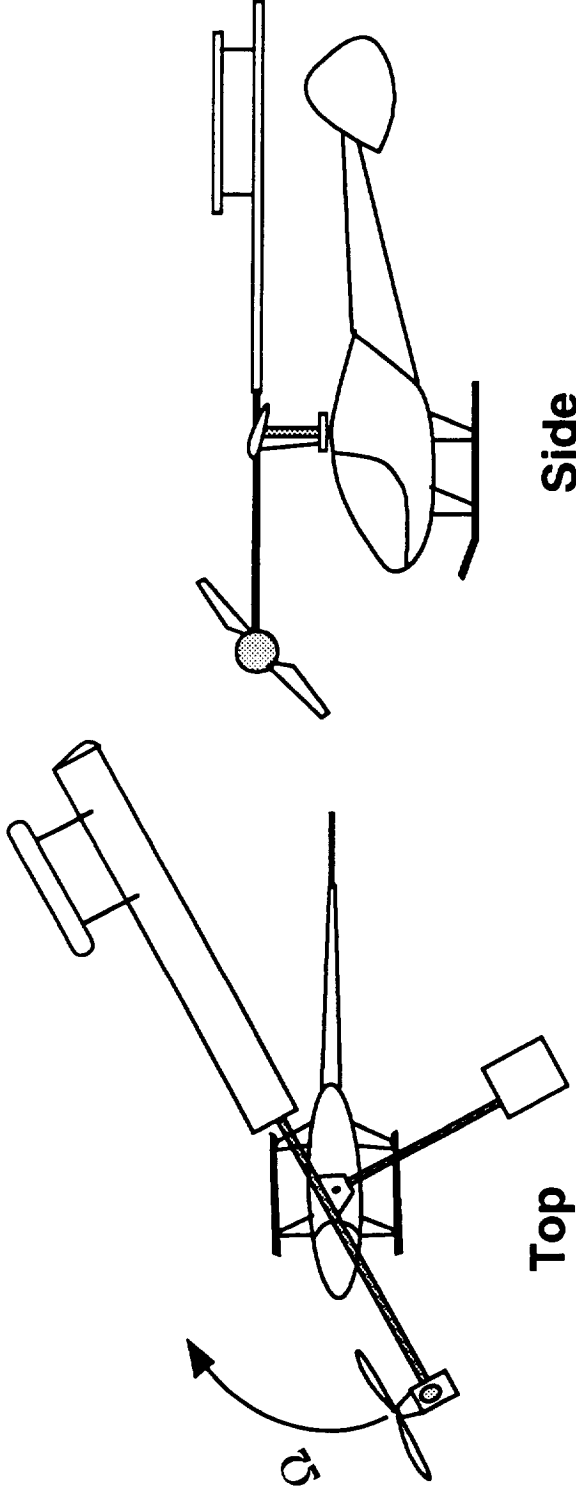
Mars Entry Vehicle



- Deploy sensors on the surface of mars
- Released after orbital entry at high altitude
- More robust than parachute
- Sensor can see sky during descent
- Not as sensitive to surface wind after landing

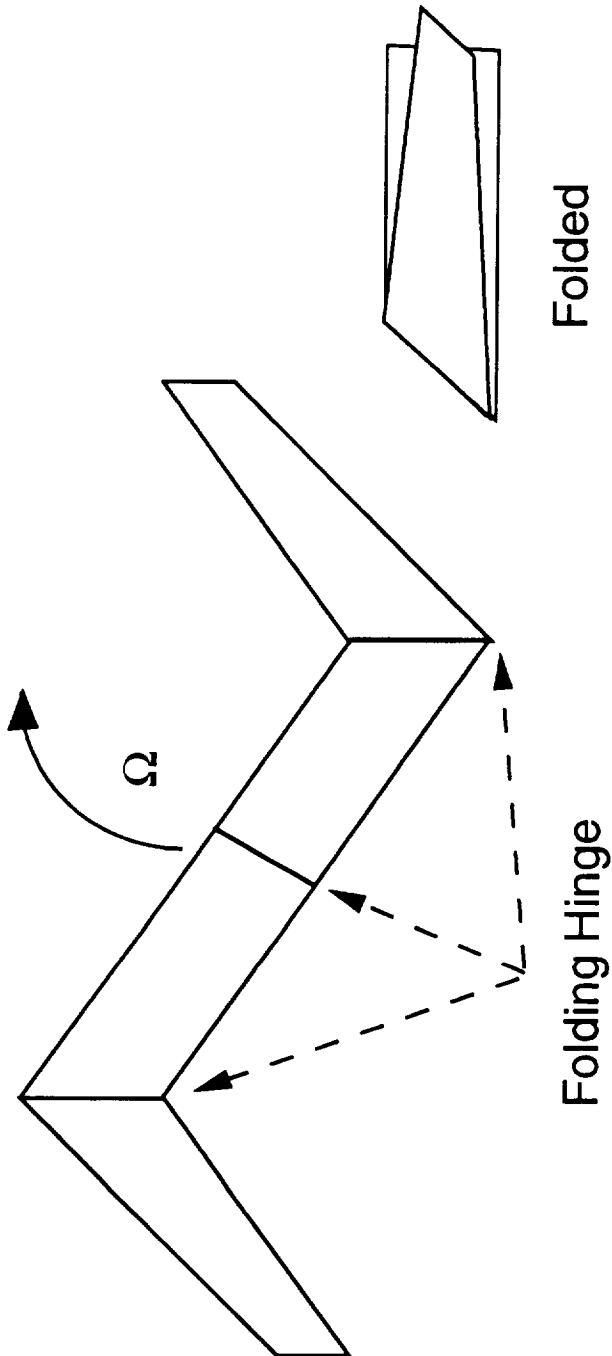
Possible Applications

Ultralight Helicopter



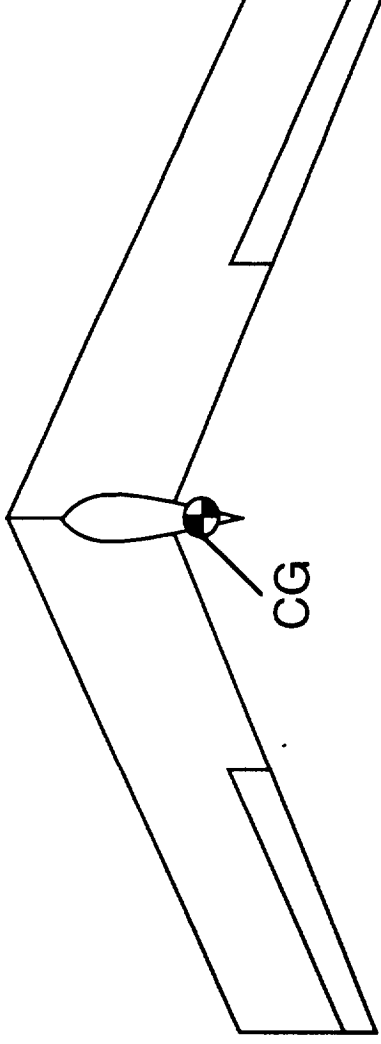
- No transmission or tail rotor required
- Automatic glide if engine fails
- Inherently stable in hover
- No license required to fly

Large Folding Autogyro

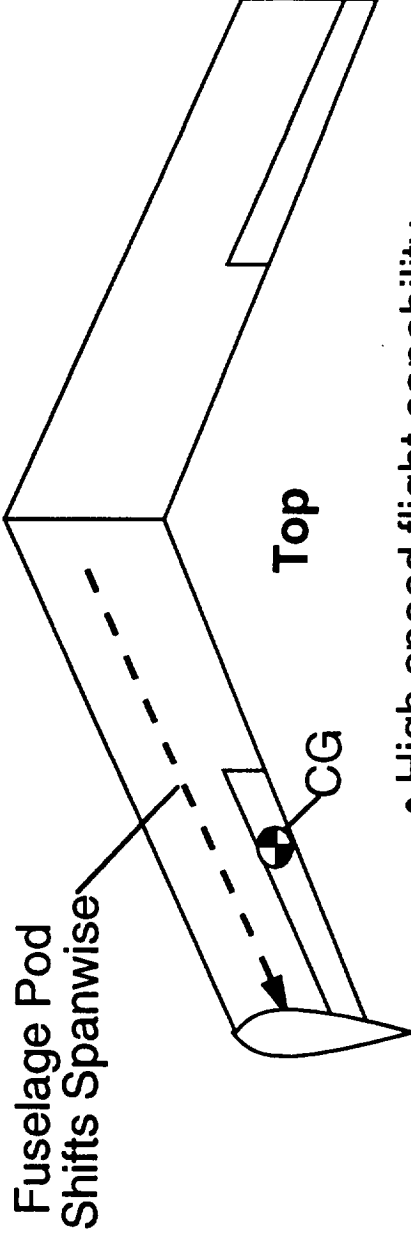


- Compact
- Easily deployed
- Purpose?

Conversion Aircraft



Swept Wing Tailless Aircraft



- High speed flight capability
- Vertical landing
- Demonstrates conversion from aircraft to autogyro with single wing
- Purpose ?

Conclusions

- Seeds are very efficient and stable fliers
- Sinking speed of seeds depends more on induced losses than parasite drag
- A simple nonlinear 6DOF simulation can model the dynamic stability and transition of autorotating seeds
- Feathering axis stability is dominated by gyroscopic effects and requires a precise and proper mass distribution
- Innovations found in modern helicopter rotors are found in maple seeds, but in disguised form
- The study of single-wing autorotation can provide insight into modern rotorcraft design problems